

This article was downloaded by:[Bochkarev, N.]
On: 11 December 2007
Access Details: [subscription number 746126554]
Publisher: Taylor & Francis
Informa Ltd Registered in England and Wales Registered Number: 1072954
Registered office: Mortimer House, 37-41 Mortimer Street, London W1T 3JH, UK



Astronomical & Astrophysical Transactions

The Journal of the Eurasian Astronomical Society

Publication details, including instructions for authors and subscription information:
<http://www.informaworld.com/smpp/title~content=t713453505>

THE STRUCTURE OF SINGULARITIES ARISING IN THE COURSE OF THE NEWTONIAN COLLAPSE OF THE DUST-LIKE MATTER

V. A. Koutvitsky^a; E. M. Maslov^a

^a Institute of Terrestrial Magnetism, Ionosphere and Radiowave Propagation RAS (IZMIRAN), 142190, Troitsk, Moscow region, Russia.

Online Publication Date: 01 January 2002

To cite this Article: Koutvitsky, V. A. and Maslov, E. M. (2002) 'THE STRUCTURE OF SINGULARITIES ARISING IN THE COURSE OF THE NEWTONIAN COLLAPSE OF THE DUST-LIKE MATTER', *Astronomical & Astrophysical Transactions*, 21:4, 197 - 216

To link to this article: DOI: 10.1080/10556790215595

URL: <http://dx.doi.org/10.1080/10556790215595>

PLEASE SCROLL DOWN FOR ARTICLE

Full terms and conditions of use: <http://www.informaworld.com/terms-and-conditions-of-access.pdf>

This article maybe used for research, teaching and private study purposes. Any substantial or systematic reproduction, re-distribution, re-selling, loan or sub-licensing, systematic supply or distribution in any form to anyone is expressly forbidden.

The publisher does not give any warranty express or implied or make any representation that the contents will be complete or accurate or up to date. The accuracy of any instructions, formulae and drug doses should be independently verified with primary sources. The publisher shall not be liable for any loss, actions, claims, proceedings, demand or costs or damages whatsoever or howsoever caused arising directly or indirectly in connection with or arising out of the use of this material.



THE STRUCTURE OF SINGULARITIES ARISING IN THE COURSE OF THE NEWTONIAN COLLAPSE OF THE DUST-LIKE MATTER

V. A. KOUTVITSKY* and E. M. MASLOV

*Institute of Terrestrial Magnetism, Ionosphere and Radiowave Propagation RAS (IZMIRAN),
142190, Troitsk, Moscow region, Russia*

(Received 11 April 2001)

We re-examine the spherically-symmetric collapse of the nonuniformly distributed dust-like cold matter. The necessary and sufficient condition for the shell-crossing spherical singularity arising is rigorously derived. The system of algebraic equations is obtained which determines the instant of appearance of the singular sphere and its radius. The explicit asymptotic solutions in the Eulerian variables describing the structure of the point-like central and spherical shell-crossing primordial singularities are found. Multiplication of flows arising after splitting the first shell-crossing singularity is investigated numerically.

Keywords: Gravitation; Hydrodynamics; Dust matter; Collapse; Large-scale structure of Universe

1 INTRODUCTION

Owing to the Jeans instability the self-gravitating interstellar gas tends to break up into separate lumps. At the non-linear stage of the instability the gas lumps collapse forming protostars (see, *e.g.*, Spitzer, 1978). The similar processes occur at formation of star clusters from ‘gas’ of stars, clusters of galaxies from ‘gas’ of galaxies and so on, up to the formation of the large-scale structure of the Universe (Pibbles, 1980; Zel’dovich and Novikov, 1983; Shandarin, Doroshkevich and Zel’dovich, 1983).

It is well known that for sufficiently large gas lumps the dynamics of the collapse is mainly determined by the gravity, so that in the first approximation one can neglect the pressure (Zel’dovich and Novikov, 1983). Obviously, the gas of stars or galaxies can be also treated as a pressureless dust-like medium. The same is true for the non-baryonic dark matter which plays a leading part in formation of the large-scale cosmic structures (Shandarin *et al.*, 1983; Gurevich, Zybin and Sirota, 1997).

In the present paper we consider evolution of an isolated self-gravitating cloud. The characteristic size of the cloud is assumed to be sufficiently large to neglect the effect of pressure, but, at the same time, sufficiently small compared with the horizon, which means we can

* Corresponding author. E-mail: zheka@izmiran.rssi.ru

ignore the cosmological expansion and validity of the Newtonian approximation. The dynamics of such a cloud is described by the equations

$$\begin{aligned}\frac{\partial \mathbf{v}}{\partial t} + (\mathbf{v} \nabla) \mathbf{v} &= -\nabla \varphi, \\ \frac{\partial \rho}{\partial t} + \operatorname{div}(\rho \mathbf{v}) &= 0, \\ \Delta \varphi &= 4\pi G \rho.\end{aligned}\tag{1}$$

Here $\mathbf{v}(\mathbf{r}, t)$ and $\rho(\mathbf{r}, t)$ are the velocity and the density of matter, $\varphi(\mathbf{r}, t)$ is the gravitational potential.

As is known, in the course of the gravitational contraction of an inhomogeneous dust cloud the singularities occur at the centre of the cloud or on some caustic surface (Zel'dovich and Novikov, 1983; Pibbles, 1980; Shandarin *et al.*, 1983). Such singularities also arise in the general relativistic dust collapse described by the Tolman solution (Papapetrou and Hamoui, 1967; Newman, 1986; Dwivedi and Joshi, 1997). The present paper is devoted to the detailed investigation of the structure of these singularities in the framework of the Eqs. (1), as well as to establishing the conditions for their formation. With the help of qualitative analysis these conditions were previously formulated by Hunter (1962). In our paper we derive them rigorously, using the properties of a two-dimensional surface determined by an implicit solution of the Eqs. (1) in the spherically-symmetric case. As to the structure of singularities, the first investigation was pursued in Penston (1969) where the singularities at the centre were considered. For this reason our main concern is with the singularities in the form of caustic spheres arising from the shell-crossing. Nevertheless, we show that the solution obtained by Penston (1969) for the central singularity is not complete because of the absence of the terms which can be of the same order as the kept ones.

The knowledge of the structure of the singularities plays a leading part in determining the general picture of matter distribution in the Universe. In the papers of Gurevich and Zybin (1988; 1995) the singularities of the central type were considered as primordial in developing the theory of non-dissipative gravitational turbulence. By hypothesis of the authors, the multiflow motion arising after formation of the first point-like singularity at the centre gives rise to a stationary dynamical structure. The motion and interaction of these structures, having different velocities and scales, result in formation of a turbulent state determining the hierarchy of the cosmic clustering. From this viewpoint the motion and interaction of the shell-crossing singularities can determine the cellular structure of the Universe observed at the superscales (Shandarin *et al.*, 1983; Gurevich and Zybin, 1995).

Finally, note the following. It is known that the spherically-symmetric collapse of a dust cloud is unstable in respect to both azimuthal perturbations (Lin, Mestel and Shu, 1965) and formation of small-size fragments with enhanced density (Hunter, 1962; 1964; Mestel, 1965). We assume that the processes of formation of the singularities we consider proceed much faster than these instabilities develop. For example, this takes place for initial distributions having well-defined maxima of the density (at the centre or on a spherical shell).

Taking the above into account, we first reconsider the general dynamics of formation of the singularities from an initial smooth distribution of dust-like matter (Section 2). We derive rigorously the conditions under which the singularities of the each kind occur. In Section 3 the explicit asymptotic solution describing in Eulerian variables the primary structure of the central singularity is found. Similarly, the solution for the spherical shell-crossing singularity is found in Section 4. In Section 5, equations describing the multiflow motion are obtained. Based on these equations the multiplication of flows arising just after splitting the first

shell-crossing singularity is investigated numerically. In Section 6 we summarize the obtained results and show that they are also applicable to the ellipsoidal distributions.

2 FORMATION OF SINGULARITIES: GENERAL ANALYSIS

In the spherically-symmetric case the system (1) becomes

$$\frac{\partial v}{\partial t} + v \frac{\partial v}{\partial r} = -\frac{Gm}{r^2}, \quad (2)$$

$$\frac{\partial \rho}{\partial t} + \frac{1}{r^2} \frac{\partial}{\partial r} (r^2 \rho v) = 0, \quad (3)$$

$$m = 4\pi \int_0^r \rho r^2 dr, \quad (4)$$

where $m(r, t)$ is a mass enclosed in a sphere of the radius r .

Since $\partial m / \partial t + v \partial m / \partial r = 0$, the Eq. (2) is easily integrated in Lagrangian variables (see, e.g., Spitzer, 1978). Obviously, the first integral is

$$H = \frac{v^2}{2} - \frac{Gm}{r}, \quad (5)$$

where $H(m)$ is an arbitrary function of m . It is determined by the initial values (say, at $t = 0$) of the coordinate $r(m, 0)$ and the velocity $v(m, 0)$ of the given infinitesimally thin layer m . The function $r(m, 0)$ is the inverse of $m(r, 0)$ and is determined by the initial mass distribution, in accordance with (4).

Integration of (5) gives rise to a relationship between r , t and m . For the motion to the centre it can be written in the form

$$F(z(m, t)) + \frac{|2H(m)|^{3/2}}{2Gm} t = F(z(m, 0)), \quad (6)$$

where

$$F(z) = \arcsin z - z(1 - z^2)^{1/2} \quad (H \leq 0), \quad (7)$$

$$F(z) = -\operatorname{arsh} z + z(1 + z^2)^{1/2} \quad (H > 0), \quad (8)$$

$$z(m, t) = \left(\frac{|H(m)| r(m, t)}{Gm} \right)^{1/2} \quad (9)$$

It should be emphasized that the Eqs. (2)–(4) and, hence, the solution (6) are valid only in that space-time region where the falling layers do not cross each other.

In the coordinates r , t , m the solution (6) describes a two-dimensional surface. To obtain the solution in Eulerian variables one needs to resolve (6) with respect to m . Evidently, this is generally impossible. Nevertheless, we can obtain some characteristic features of the motion knowing the structure of the surface (6) only, without an explicit formula for $m(r, t)$. In particular, it turns out to be possible to find the formulas determining the instant of

appearance of the spherical shell-crossing singularity and its radius for rather general initial conditions.

Let us consider a spherical dust cloud having a finite mass M . We assume that initially, at $t = 0$, the cloud was at rest and had a mass distribution $\rho(r, 0)$ vanishing at infinity. Then $H = -Gm/r(m, 0) \leq 0$, so that

$$v^2 = \frac{2Gm}{r}(1 - z^2), \quad (10)$$

$$0 \leq z = \left[\frac{r(m, t)}{r(m, 0)} \right]^{1/2} \leq 1. \quad (11)$$

Hence, in accordance with (7), $F(z(m, 0)) = F(1) = \pi/2$, and the Eq. (6) becomes

$$t = \sigma(m, z) \equiv t_f(m) \left[1 - \frac{2}{\pi} F(z) \right], \quad (12)$$

where

$$t_f(m) = \frac{\pi r^{3/2}(m, 0)}{2(2Gm)^{1/2}} \quad (13)$$

The quantity $t_f(m)$ has the sense of the time needed for a given layer m to fall down on the centre (provided that the shell-crossing does not occur). For the considered non-singular initial distributions with non-zero density at the centre the function $t_f(m)$ does not become zero and remains finite in the range $0 \leq m < M$.

The solution $r(m, t)$ of the Eq. (12) is a t -parameterized family of contour lines of the surface $\sigma(m, z)$ considered over the plane (m, r) (Fig. 1). The singularity appears at that instant and at that point where $r^2 \partial r / \partial m \sim 1/\rho$ becomes zero.

Differentiating (12) with respect to m and taking into account that

$$\frac{dF}{dz} = \frac{2z^2}{(1 - z^2)^{1/2}}, \quad (14)$$

$$\frac{\partial z}{\partial m} = \frac{z}{6m} \left[3m \frac{\partial}{\partial m} \ln r(m, t) - Y(m) \right], \quad (15)$$

$$\frac{dt_f}{dm} = \frac{t_f(m)}{2m} [Y(m) - 1], \quad (16)$$

$$Y(m) = 3m \frac{\partial}{\partial m} \ln r(m, 0), \quad (17)$$

we get

$$r^2 \frac{\partial r}{\partial m} = \frac{4G}{\pi^2} t_f^2(m) z^3 \left[\frac{2}{3} z^3 - (1 - Y(m)) \left(z - \frac{z^3}{3} + (1 - z^2)^{1/2} \arccos z \right) \right]. \quad (18)$$

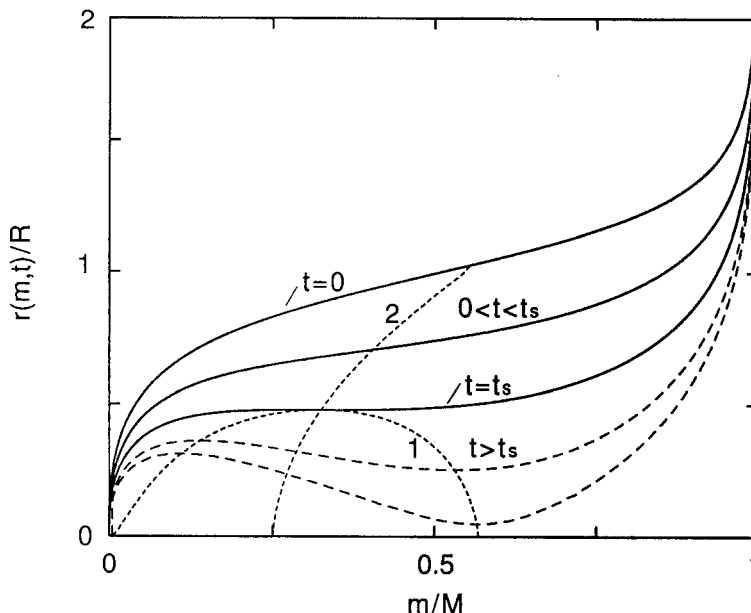


FIGURE 1 The Lagrangian particles (spherical layers) falling in accordance with the solution (12). The initial conditions are $v(r, 0) = 0$, $\rho(r, 0) = (1 + 5r^5)/(1 + r^8)^2$. The axes are normalized to the total mass M and the averaged radius R of the matter distribution, $R = (4\pi/M) \int_0^\infty \rho(r, 0)r^3 dr$. The curves 1, 2 (indicated by a short dash) are determined by the Eqs. (24), (26), correspondingly.

The right hand side of (18) becomes zero when z or/and squared brackets become zero. Let us suppose, first, that for a given initial matter distribution

$$Y(m) \geq 1 \quad (0 \leq m < M). \tag{19}$$

Then (18) becomes zero only if $z = 0$, *i.e.*, in accordance with (11), (12), when $r = 0$, $t = t_f(m)$. This implies that under the condition (19) the singularity appears at the centre only. Indeed, as is seen from (16), $t_f(m)$ does not decrease with increasing m . Therefore, all layers reach the centre one after another, and without crossing each other, the layer with infinitesimally small mass being the first. From this it follows that the singularity at the centre appears at the instant

$$t_s = t_f(0) = \left(\frac{3\pi}{32G\rho(0, 0)} \right)^{1/2} \tag{20}$$

This fact is well-known for monotonically decreasing mass distributions (see, *e.g.*, Hunter, 1962). We show that this is also true for some non-monotonic distributions. Indeed, the condition (19) can be rewritten as

$$\int_0^r \frac{\partial \rho(r, 0)}{\partial r} r^3 dr \leq 0 \quad (0 \leq r < \infty). \tag{21}$$

This inequality is obviously fulfilled for monotonically decreasing $\rho(r, 0)$. It is clear, however, that it can also be fulfilled for some initial distributions having, besides the mandatory

maximum at the centre, other local maxima. Physically, this means that, despite the non-monotonicity of $\rho(r, 0)$, all layers do have a chance to reach the centre without crossing.

Let now there exist such m , that

$$Y(m) < 1, \quad (22)$$

or, correspondingly, such r , that

$$\int_0^r \frac{\partial \rho(r, 0)}{\partial r} r^3 dr > 0. \quad (23)$$

Then the expression in the squared brackets in (18) becomes zero when

$$Y(m) = P(z), \quad (24)$$

where

$$P(z) = \frac{z - z^3 + (1 - z^2)^{1/2} \arccos z}{z - z^3/3 + (1 - z^2)^{1/2} \arccos z}. \quad (25)$$

On the plane (m, z) the Eq. (24) determines a curve $z = z(m)$. On the plane (m, r) this curve is a point set $r = r(m)$ of extrema of the t -parametrized family of curves $r(m, t)$ considered formally in the range $t > t_s$. In Figure 1 these curves $r(m, t)$ are depicted by dashed lines, in order to emphasize a failure of Eqs. (2)–(4) in describing the layer dynamics at $t > t_s$ in the whole space (see Section 5). In accordance with (12), the instants t_s , at which the singularities appear, are the minimal values of the function $\sigma(m, z)$ on the curve $z = z(m)$. Thus, the singularities arise at those layers m_s , where $d\sigma(m, z(m))/dm = 0$, $d^2\sigma(m, z(m))/dm^2 > 0$. On the plane (m, r) this corresponds to the maxima of the function $r = r(m)$ (curve 1 in Fig. 1, as an illustration).

Calculating the first derivative of $\sigma(m, z(m))$ with respect to m and equating it to zero, one obtains

$$m(\ln Y(m))' = -\frac{z}{6}P'(z) \quad (26)$$

(hereinafter the primes mean derivatives with respect to an indicated argument). In deriving (26) we have used the Eq. (24), the expression for $z'(m)$,

$$z' = \frac{Y'}{P'}, \quad (27)$$

and the identity

$$\frac{\pi/2 - F}{F'} = \frac{zP}{3(1 - P)}. \quad (28)$$

The Eq. (26) determines a curve $z = \tilde{z}(m)$ (in Fig. 1 the example of such a curve is marked off by 2). The plots of $P(z)$ and $-(z/6)P'(z)$ are shown in Figure 2.

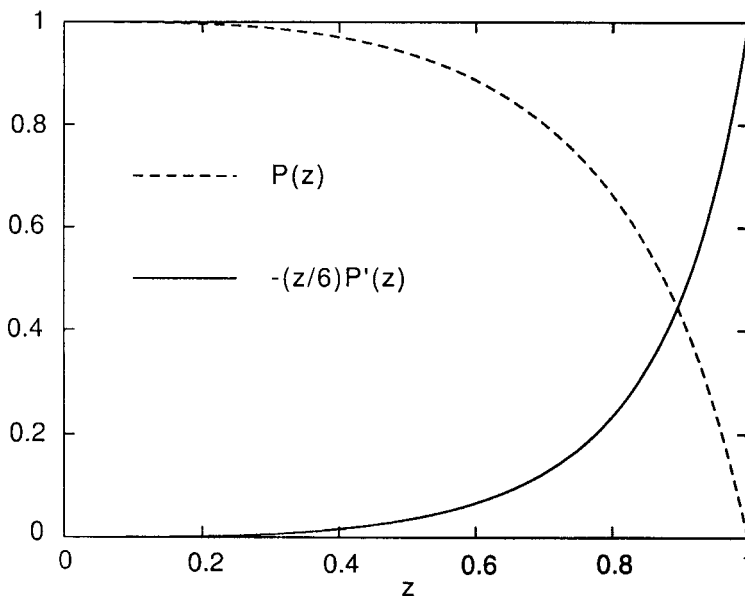


FIGURE 2 The dependance on z of the right hand sides of the Eqs. (24), (26). For the chosen initial conditions the solution of the Eqs. (24), (26) (the intersection point of the curves 1 and 2 in Fig. 1) is $m_s = 0.325 M$, $z_s = 0.736$. In accordance with (32), (33) this gives $t_s = 1.28 R^{3/2} (GM)^{-1/2}$, $r_s = 0.48 R$.

For a given initial matter distribution the Eqs. (24), (26) constitute a set of algebraic equations determining the points on the plane (m, z) where the singularities can arise. Let $(m_s, z_s = z(m_s))$ be one of these points. We calculate now the second order derivative of $\sigma(m, z)$ along the curve $z = z(m)$ and require its positivity. In calculation we use the formulas (27), (28), the expression

$$z'' = \frac{Y''}{P'} - \frac{Y'^2 P''}{P'^3} \tag{29}$$

and the identity

$$-\frac{F''}{F'} = \frac{P'}{P(1-P)} + \frac{3-2P}{zP}. \tag{30}$$

If, in addition, Eqs. (24), (26) are taken into account, the resulting inequality can be written as

$$36[m(m(\ln Y)')]_{m_s} > [zP(zP')]_{z_s}. \tag{31}$$

Thus, if (m_s, z_s) is a solution of the set (24), (26) and satisfies (31), then at the instant

$$t_s = \sigma(m_s, z_s) = \frac{2}{\pi} t_f(m_s) [z_s(1-z_s^2)^{1/2} + \arccos z_s] \tag{32}$$

the density becomes infinite on a sphere of the radius

$$r_s = z_s^2 r(m_s, 0). \quad (33)$$

The inequality (22) (or, interchangeably, (23)) is the necessary and sufficient condition for arising the spherical shell-crossing singularity. A rigorous proof of this statement is given in the Appendix. The physical meaning of the condition (22) is clear. Indeed, as is seen from (16), $t_f(m)$ decreases with increasing m over those intervals where (22) holds. Therefore, the farther away a layer is the smaller is the time it takes to fall to the centre. This obviously leads to the crossings of the layers, the first one happening at $t = t_s, r = r_s$. The singular sphere, arising at this instant, splits immediately into two singular spheres which continue to contract. In the interspace between them the three-flow motion takes place, so that the standard hydrodynamic Eqs. (2)–(4) are invalid there. In Section 5 we derive equations, governing the dynamics of the layers in the multiflow regions, and also give results of the numerical integration. But before that, in the next two Sections, we investigate the structure of the primordial singularities, arising at $t = t_s$.

Note that potentially it is possible for several singularities to occur at different instants t_s and with different radii r_s , the Eqs. (24), (26) can formally have several solutions corresponding to the minima of the function $\sigma(m, z(m))$. However, this possibility does not imply that all singularities do really occur, because certain of the layers m_s can find themselves in a multiflow region (formed, *e.g.*, due to the splitting of a primordial singularity arising before) in a time smaller than t_s for a given layer. For example, if for an initial mass distribution the time of appearance of the shell-crossing singularity (32) is smaller than the time of appearance of the central singularity (20), then for this distribution the multiflow region can reach the centre before the conventional singularity at the centre forms. In this case the density at the centre becomes infinite in a time smaller than t_s (20), just due to the lower boundary of the multiflow region falling at the centre.

3 THE STRUCTURE OF THE PRIMORDIAL SINGULARITY ARISING AT THE CENTRE

Let us consider the initial matter distribution having an enhanced density near the centre, so that for small r

$$\frac{\rho(r, 0)}{\rho(0, 0)} = 1 - \xi^2 + O(\xi^4), \quad (34)$$

where

$$\xi = \frac{r}{r_0}, \quad r_0 = \left| \frac{2\rho(0, 0)}{\rho''(0, 0)} \right|^{1/2}, \quad (35)$$

r_0 is the characteristic scale of an inhomogeneity.

To determine the structure of the singularity in the Eulerian coordinates r, t one should resolve the Eq. (12) with respect to m assuming that m and z are small and t is close to t_s (20). Introducing the dimensionless variables

$$\tau = \frac{t}{t_s}, \quad \mu = \frac{m(r, t)}{(4\pi/3)r_0^3\rho(0, 0)}, \tag{36}$$

when $\xi^2 \ll 1, \mu^{2/3} \ll 1, z^2 \ll 1$ one has

$$\begin{aligned} r(m, 0) &= r_0\mu^{1/3} \left[1 + \frac{1}{5}\mu^{2/3} + O(\mu^{4/3}) \right], \\ t_f(m) &= t_s \left[1 + \frac{3}{10}\mu^{2/3} + O(\mu^{4/3}) \right], \\ F(z) &= \frac{2}{3}z^3 \left[1 + \frac{3}{10}z^2 + O(z^4) \right], \\ z^2 &= \frac{\xi}{\mu^{1/3}} \left[1 - \frac{1}{5}\mu^{2/3} + O(\mu^{4/3}) \right]. \end{aligned} \tag{37}$$

With these formulas the Eq. (12) becomes

$$\frac{4\xi^{3/2}}{3\pi\mu^{1/2}} \left[1 + \frac{3}{10}z^2 + O(z^4) \right] = 1 - \tau + \frac{3}{10}\mu^{2/3} + O(\mu^{4/3}). \tag{38}$$

Suppose, first, that in the right hand side of (38) $\mu^{2/3} \ll 1 - \tau$. Then, in the first approximation, we find

$$\mu \approx \frac{16\xi^3}{9\pi^2(1 - \tau)^2}. \tag{39}$$

With this result it is seen from (37), that $z^2 \sim (1 - \tau)^{2/3}$. Hence, our assumption is justified in the region

$$\xi^{4/7} \ll (1 - \tau)^{2/3} \ll 1, \tag{40}$$

where, evidently, $z^2 \ll 1, \xi^2 \ll \mu^{2/3} \ll 1 - \tau \ll 1$.

Consider the next approximation assuming the condition (40) is fulfilled. Magnitudes of the terms in (38) are now estimated with the help of (39). As a result, we obtain

$$\mu = \frac{16\xi^3}{9\pi^2(1 - \tau)^2} [1 + \varepsilon(\xi, \tau) + O(\varepsilon^2)], \tag{41}$$

where

$$\varepsilon(\xi, \tau) = \frac{3}{5} \left(\frac{3\pi}{4} \right)^{2/3} (1 - \tau)^{2/3} - \frac{3}{5} \left(\frac{3\pi}{4} \right)^{-4/3} \frac{\xi^2}{(1 - \tau)^{7/3}}. \tag{42}$$

Let now

$$(1 - \tau)^{2/3} \ll \xi^{4/7} \ll 1. \quad (43)$$

In this region in the first approximation the Eq. (38) gives

$$\mu \approx \left(\frac{40}{9\pi}\right)^{6/7} \xi^{9/7}. \quad (44)$$

In the next approximation we use (44) and the fact that in the region (43) $z^2 \sim \xi^{4/7}$. Thus, we get

$$\mu = \left(\frac{40}{9\pi}\right)^{6/7} \xi^{9/7} [1 + \delta(\xi, \tau) + O(\delta^2, \xi^{6/7})], \quad (45)$$

where

$$\delta(\xi, \tau) = \frac{9}{35} \left(\frac{9\pi}{40}\right)^{2/7} \xi^{4/7} - \frac{20}{7} \left(\frac{9\pi}{40}\right)^{4/7} \frac{1 - \tau}{\xi^{6/7}}. \quad (46)$$

With the found mass μ the density and the velocity of the matter are determined by the formulas (4), (10), (35)–(37). Introducing the characteristic velocity $v_0 = r_0/t_s$ we finally obtain

$$\frac{\rho(r, t)}{\rho(0, 0)} = \frac{16}{9\pi^2(1 - \tau)^2} \left[1 + \frac{3}{5} \left(\frac{3\pi}{4}\right)^{2/3} (1 - \tau)^{2/3} - \left(\frac{3\pi}{4}\right)^{-4/3} \frac{\xi^2}{(1 - \tau)^{7/3}} + O(\varepsilon^2) \right], \quad (47)$$

$$\frac{v(r, t)}{v_0} = -\frac{2\xi}{3(1 - \tau)} \left[1 - \frac{1}{5} \left(\frac{3\pi}{4}\right)^{2/3} (1 - \tau)^{2/3} - \frac{3}{10} \left(\frac{3\pi}{4}\right)^{-4/3} \frac{\xi^2}{(1 - \tau)^{7/3}} + O(\varepsilon^2) \right] \quad (48)$$

for $\xi^{4/7} \ll (1 - \tau)^{2/3} \ll 1$, and

$$\frac{\rho(r, t)}{\rho(0, 0)} = \frac{3}{7} \left(\frac{40}{9\pi}\right)^{6/7} \xi^{-12/7} \left[1 + \frac{13}{35} \left(\frac{9\pi}{40}\right)^{2/7} \xi^{4/7} - \frac{20}{21} \left(\frac{9\pi}{40}\right)^{4/7} \frac{1 - \tau}{\xi^{6/7}} + O(\delta^2, \xi^{6/7}) \right], \quad (49)$$

$$\frac{v(r, t)}{v_0} = -\frac{\pi}{2} \left(\frac{40}{9\pi}\right)^{3/7} \xi^{1/7} \left[1 - \frac{13}{35} \left(\frac{9\pi}{40}\right)^{2/7} \xi^{4/7} - \frac{10}{7} \left(\frac{9\pi}{40}\right)^{4/7} \frac{1 - \tau}{\xi^{6/7}} + O(\delta^2, \xi^{6/7}) \right] \quad (50)$$

for $(1 - \tau)^{2/3} \ll \xi^{4/7} \ll 1$.

It is easy to verify by substitution that, within the accuracy of the analysis, the expansions (47)–(50) satisfy the basic Eqs. (2)–(4). They describe in Eulerian variables the structure of the solution near the centre. The leading terms of the expansions were obtained by Penston (1969). Also, the third term of (47) was written down there (but unfortunately, with an erroneous numerical coefficient), however in the region (40) the second terms in (47), (48) can make even greater contributions and, hence, must be taken into account. As to the second

terms in (49), (50), their role when substituting in (2)–(4) becomes important in the next approximation.

4 THE STRUCTURE OF THE PRIMORDIAL SPHERICAL SINGULARITY

Now we shall treat the right hand side of (12) as a function of m, r . Denoting $\sigma(m, r) = \sigma(m, z(m, r))$, near the singular sphere we can write the expansion

$$\begin{aligned}
 t - t_s - \left(\frac{\partial\sigma}{\partial r}\right)_s (r - r_s) &= \frac{1}{2} \left(\frac{\partial^2\sigma}{\partial r^2}\right)_s (r - r_s)^2 + \left(\frac{\partial^2\sigma}{\partial r\partial m}\right)_s (r - r_s)(m - m_s) \\
 &+ \frac{1}{6} \left(\frac{\partial^3\sigma}{\partial m^3}\right)_s (m - m_s)^3 + \frac{1}{24} \left(\frac{\partial^4\sigma}{\partial m^4}\right)_s (m - m_s)^4 \\
 &+ O((r - r_s)^3, (r - r_s)^2(m - m_s), (r - r_s)(m - m_s)^2). \quad (51)
 \end{aligned}$$

Here we took into account that

$$\left(\frac{\partial\sigma}{\partial m}\right)_s = 0, \quad \left(\frac{\partial^2\sigma}{\partial m^2}\right)_s = 0$$

because of (24), (26) and hence kept the terms of the third and fourth orders in $m - m_s$. Using again (24), (26) and the identity

$$zP' = -(1 - P)\left(3 + \frac{z^2P}{1 - z^2}\right)$$

for the remaining derivatives we obtain

$$\begin{aligned}
 \left(\frac{\partial\sigma}{\partial r}\right)_s &= \frac{1}{v_s}, \\
 \left(\frac{\partial^2\sigma}{\partial r^2}\right)_s &= \frac{1}{2r_s v_s (1 - z_s^2)}, \\
 \left(\frac{\partial^2\sigma}{\partial r\partial m}\right)_s &= \frac{1}{6m_s v_s} \left(\frac{zP'}{1 - P}\right)_s, \\
 \left(\frac{\partial^3\sigma}{\partial m^3}\right)_s &= \frac{t_s}{2m_s^3} \left[m(m(\ln Y)')' - \frac{1}{36} zP(zP')' \right]_s, \\
 \left(\frac{\partial^4\sigma}{\partial m^4}\right)_s &= \frac{t_s}{2m_s^4} \left[m(m(m(\ln Y)')')' + \frac{1}{216} zP(zP(zP')')' \right]_s \\
 &- \frac{6}{m_s} \left(\frac{\partial^3\sigma}{\partial m^3}\right)_s \left(1 - \frac{1}{36} zP'\right)_s. \quad (52)
 \end{aligned}$$

Here

$$v_s = - \left[\frac{2Gm}{r} (1 - z^2) \right]_s^{1/2} \quad (53)$$

is the velocity of the singular sphere at the instant $t = t_s$ (32) it arises. The functions $Y(m)$ and $P(z)$ are defined in (17), (25). The label s indicates that a quantity is taken at $m = m_s$, $r = r_s$, $z = z_s$. Recall that the primes denote the derivatives with respect to m or z .

Suppose that in the right hand side of (51) the term $\sim (m - m_s)^3$ is the leading one.

Then, in the first approximation

$$(m - m_s)^3 \approx \frac{6t_s}{(\partial^3 \sigma / \partial m^3)_s} \Delta, \quad (54)$$

$$\Delta(r, t) = \frac{r_s - r - v_s(t_s - t)}{v_s t_s}. \quad (55)$$

Note that, according to (31), the quantity $(\partial^3 \sigma / \partial m^3)_s$ is always positive (see (52)), as it must in agreement with the physical meaning of (54).

Using (54) it is easy to check that the term $(m - m_s)^3$ plays a leading part in the region

$$\left| 1 - \frac{r}{r_s} \right|^{1/2} \ll |\Delta|^{1/3} \ll 1. \quad (56)$$

Consider the next approximation assuming the condition (56) is satisfied. Taking account of the terms $(r - r_s)(m - m_s)$ and $(m - m_s)^4$ one finds

$$m - m_s = \left(\frac{6t_s}{\partial^3 \sigma / \partial m^3} \right)_s^{1/3} \Delta^{1/3}(r, t) [1 + \eta(r, t) + O(\eta^2)], \quad (57)$$

$$\eta(r, t) = \frac{1}{12} \left(\frac{6t_s}{\partial^3 \sigma / \partial m^3} \right)_s^{1/3} \left[\frac{4r_s}{t_s} \left(\frac{\partial^2 \sigma}{\partial r \partial m} \right)_s \frac{1 - r/r_s}{\Delta^{2/3}} - \left(\frac{\partial^4 \sigma / \partial m^4}{\partial^3 \sigma / \partial m^3} \right)_s \Delta^{1/3} \right]. \quad (58)$$

Differentiating (57), (58) with respect to r we finally obtain the expression for the density in the region (56):

$$\rho(r, t) = \frac{\gamma_s}{4\pi r^2 \Delta^{2/3}} \left[1 - \alpha_s \frac{1 - r/r_s}{\Delta^{2/3}} - \beta_s \Delta^{1/3} + O(\eta^2) \right], \quad (59)$$

where the constants $\alpha_s, \beta_s, \gamma_s$ are calculated with the help of (52)–(53) by the formulas

$$\begin{aligned}\alpha_s &= r_s |v_s| \gamma_s \left(\frac{\partial^2 \sigma}{\partial r \partial m} \right)_s, \\ \beta_s &= 3 t_s v_s^2 \gamma_s \left[\left(\frac{\partial^2 \sigma}{\partial r \partial m} \right)_s + \frac{3}{4} t_s^2 v_s^2 \gamma_s^3 \left(\frac{\partial^4 \sigma}{\partial m^4} \right)_s \right], \\ \gamma_s &= \frac{1}{3 |v_s| t_s} \left(\frac{6 t_s}{\partial^3 \sigma / \partial m^3} \right)_s^{1/3}.\end{aligned}\quad (60)$$

With (57) the velocity follows from (10):

$$v(r, t) = v_s \left[1 + \frac{3 t_s |v_s|}{r_s} \alpha_s \Delta^{1/3} + O(\eta^2) \right]. \quad (61)$$

At $t = t_s$ the formulas (59)–(61) describe the structure of the spherical singularity in the vicinity of r_s . It is seen that in the main order we have $\rho \sim (r - r_s)^{-2/3}$, as in the case of planar symmetry (Penston, 1969).

Figure 3 shows the dynamics of formation of the primordial spherical singularity in the interval $0 \leq t \leq t_s$ resulting from (59). For comparison the numerical solution of the starting Eq. (12) is depicted by the solid lines. As expected, the density profiles asymptotically fit together at $t \sim t_s, r \sim r_s$.

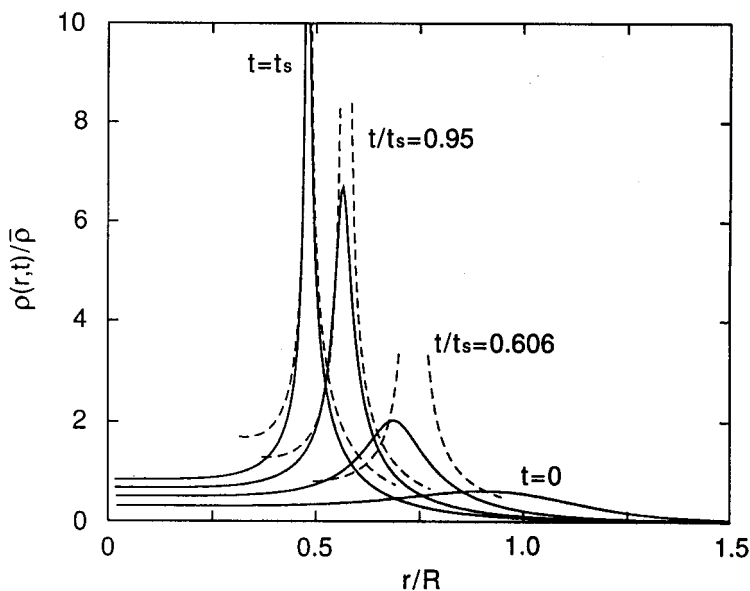


FIGURE 3 Formation of the spherical shell-crossing singularity. The initial conditions are the same as in Figure 1. The ordinate axis is normalized to the averaged density $\bar{\rho}$ of the initial distribution, $\bar{\rho} = M((4/3)\pi R^3)^{-1}$. Solid lines indicate the numerical solution of the Eq. (12), dashed lines show the asymptotic solution (59).

5 WHAT HAPPENS AT $t > t_s$?

As it was mentioned in Section 2, at $t > t_s$ a spatial region arises in which a multiflow motion takes place. Such a motion can be described by the system of hydrodynamic Eqs. (2)–(4) written down for each individual flow (Gurevich and Zybin, 1988). It turns out however that for numerical integration the system of equations in Lagrangian variables is more convenient.

Let $r(m, t)$ be the Lagrangian coordinate of an infinitesimal layer, m – its label coinciding at $t > t_s$ with the mass of a ball of radius r . The dynamics of the layer is described by the Newtonian equation,

$$\frac{\partial^2 r(m, t)}{\partial t^2} = -G \frac{\mathcal{M}(r(m, t), t)}{r^2(m, t)}. \quad (62)$$

Here $\mathcal{M}(r, t)$ is the mass determining the gravitational potential at the radius r . It is equal to the sum of the masses of the all layers having Lagrangian coordinates less than r . At $t > t_s$ the layers can intersect each other and, hence, can belong to the different flows. In this case $\mathcal{M}(r, t)$ is no longer the integral of motion and equals the mass m plus the total mass of the layers, which in the course of falling the layer m have entered into the sphere of the radius r , and minus the mass of the layers which have escaped from this sphere (see Fig. 1). Thus, for a given layer m moving in a $(2n + 1)$ -flow region one has

$$\mathcal{M}(r, t) = \sum_{j=0}^n (m_{2j+1} - m_{2j}), \quad (63)$$

where $m_i(r, t)$ ($1 \leq i \leq 2n + 1$) are the roots of the equation

$$r(m, t) = r(m_i, t), \quad (64)$$

ordered as

$$0 = m_0 \leq m_1 \leq m_2 \leq \dots \leq m_k = m \leq \dots \leq m_{2n+1}$$

Obviously, at $t < t_s$, when a one-flow motion takes place, $\mathcal{M}(r, t) = m_1 = m$.

The Eqs. (62)–(64) constitute a complete system determining the Lagrangian coordinate r of an arbitrary layer m . With the known function $r(m, t)$ the velocity of each partial flow at the point (r, t) is determined by

$$v_i = \left(\frac{\partial r}{\partial t} \right)_{m_i}, \quad (65)$$

and the total density of matter is found as the sum of all partial densities,

$$\rho = \sum_{i=1}^{2n+1} \rho_i, \quad \rho_i = \frac{1}{4\pi r^2} \left| \frac{\partial r}{\partial m} \right|_{m_i}^{-1}. \quad (66)$$

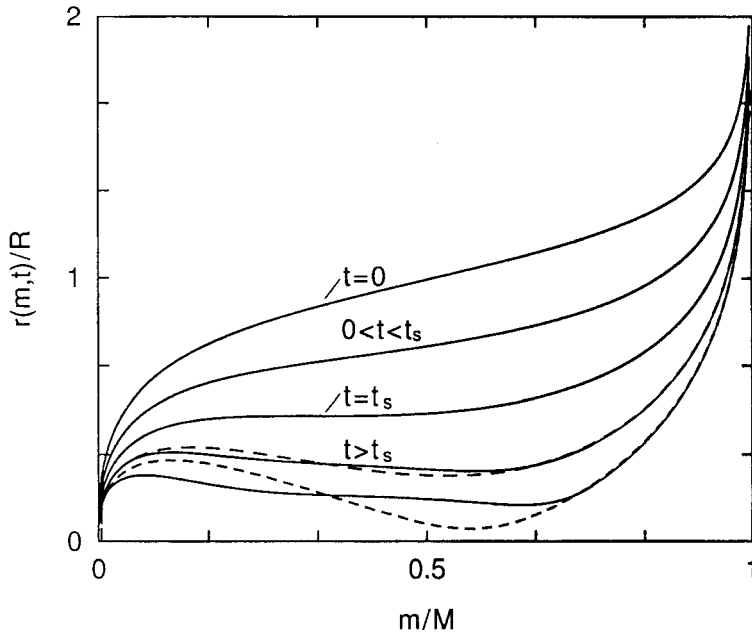


FIGURE 4 The Lagrangian particles falling in accordance with the Eqs. (62)–(64). The initial conditions and instants of time are the same as in Figure 1. For comparison the formal solutions of the Eq. (12) at $t > t_s$ are depicted (the dashed lines from Fig. 1).

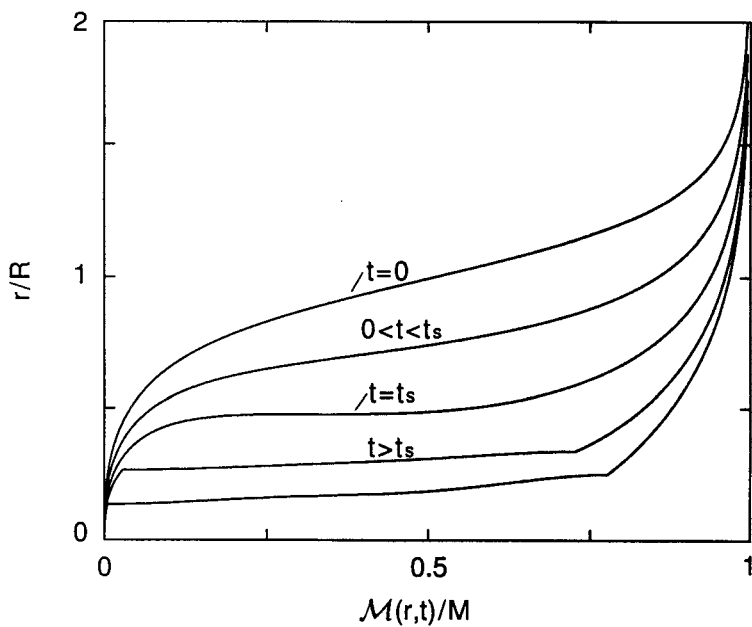


FIGURE 5 The radial distribution of the mass \mathcal{M} . The initial conditions and instants of time are the same as in Figure 1.

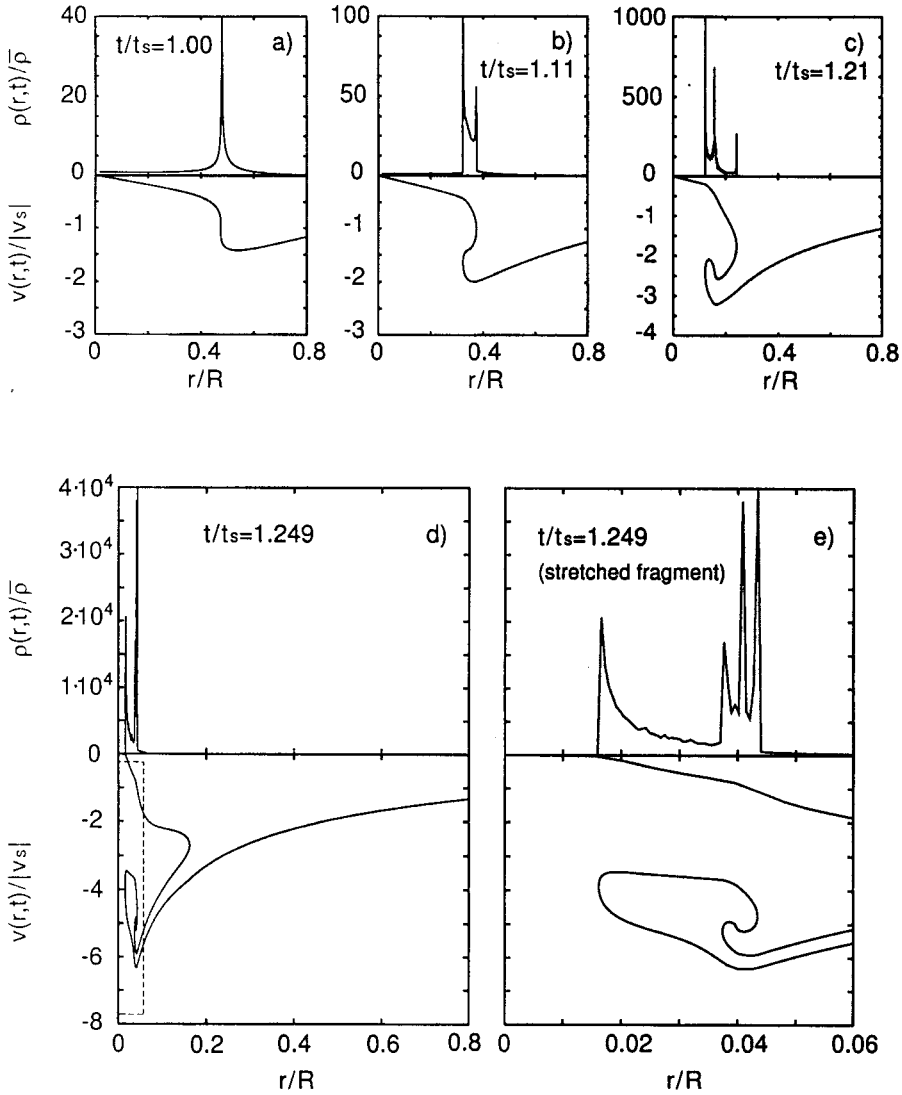


FIGURE 6 Formation of the multiflow regions in the matter falling to the centre at $t \geq t_s$.

The mass $\mathcal{M}(r, t)$ is related to the total density in the ordinary way,

$$\mathcal{M} = 4\pi \int_0^r \rho r^2 dr. \quad (67)$$

The existence theorem for the system (62)–(64) in the case of planar symmetry was recently proved by Swatton and Clarke (1998). In the present paper we report the numerical solution of this system in spherical symmetry obtained by the direct modelling of the motion of the Lagrangian particles for the discrete version of the Eq. (62). The region of integration was broken down into thin spherical layers considered as collisionless particles on a line.

Thereafter we calculated the motion of each layer in the gravitation field created by the layers arranged below the given one. The results are presented in Figures 4–6.

As one would expected, when $t \leq t_s$ the curves $r(m, t)$ in Figure 4 coincide with the corresponding curves in Figure 1. For $t > t_s$ the solution of the system (62)–(64) differs essentially from the solution of the Eq. (12) because since $t = t_s$ the gravitational potential at the radius r is generated by the mass \mathcal{M} no longer coinciding with m . In Figure 5 is presented the distribution of \mathcal{M} along the radius calculated in accordance with (62), (63). For $t > t_s$ it is seen that $\partial\mathcal{M}/\partial r \rightarrow +\infty$ at the boundaries of the multiflow region. This implies that the singular sphere arising at $t = t_s$ splits instantaneously into two singular spheres. The appearance of the three-flow motion between the spheres is well seen from the velocity distribution (Fig. 6a, b, c). In the interior of the three-flow region a new peak of the density progressively forms (Fig. 6c) which then becomes a new singular sphere. In its turn this sphere also splits into two ones with the region of the five-flow motion between them (Fig. 6d, e). The boundaries of the multiflow regions embedded into each other are determined by the condition $|dv/dr| = \infty$. From Figure 6e it is seen that in the five-flow region the formation of a new singularity begins, which will lead to the appearance of the seven-flow motion.

So, we observe the multiplication of flows already when moving the dust matter to the centre. Further development of the process will essentially depend on the model of behaviour of the matter at the centre. Thus on the assumption of the reflection of the matter from the centre it seems likely that some quasi-stationary oscillating structure arises near the centre, with the number of flows in it increasing indefinitely (Gurevich and Zybin, 1988; 1995). It may be suggested that the intersection of the shell-crossing singularities belonging to the different structures of a maximum size is responsible for the observed large-scale cellular structure of the Universe (Shandarin *et al.*, 1983).

6 CONCLUSION

The implicit solution of the hydrodynamic equations describing the spherically-symmetric collapse of a dust cloud determines some two-dimensional surface in the space of variables m, r, t . We have investigated in detail the behaviour of the contour lines of this surface on the plane m, r . As a result, we have rigorously derived the condition (22) (or, interchangeably, (23)) on the initial matter distribution under which the shell-crossing spherical singularity occurs. It turned out that this condition is both necessary and sufficient for the shell-crossing singularity arising (see Appendix). If this condition is not fulfilled, only the point-like singularity at the centre will arise. We have obtained the system of algebraic Eqs. (24), (26), the solution of which enables one to calculate the instant of appearance of the first shell-crossing singularity and the radius of the singular sphere (formulas (32), (33)). Also, we have found the explicit asymptotic solutions describing in Eulerian variables the structure of the central and spherical self-crossing singularities (formulas (47)–(50), (59)–(61)).

Further, we have obtained the system of Eqs. (62)–(64), describing the multiflow motion of the dust-like matter. With these equations we have investigated the formation of the spherical singularities in the multiflow regions. As shown in Figure 6, each new-formed spherical singularity, beginning with the primordial singularity, splits instantaneously into two new spherical singularities which become the boundaries of a new multiflow region embedded into the old one. We have observed this process up to the lower boundary of the total multiflow region falling on the centre.

Up to this point we considered the spherically-symmetric collapse. Nevertheless, all our results can be easily extended to the ellipsoidal matter distributions which seem more

realistic. For example, the matter distribution near an arbitrary maximum of the density can be written as

$$\frac{\rho}{\rho_0} = 1 + \frac{1}{2} \left[\left(\frac{\partial^2 \rho}{\partial x^2} \right)_0 x^2 + \left(\frac{\partial^2 \rho}{\partial y^2} \right)_0 y^2 + \left(\frac{\partial^2 \rho}{\partial z^2} \right)_0 z^2 \right] + \dots = 1 - \xi^2 + \dots,$$

where

$$\xi = \left(\frac{x^2}{a^2} + \frac{y^2}{b^2} + \frac{z^2}{c^2} \right)^{1/2},$$

a, b, c are constants. It easy to check (see, e.g., Gurevich and Zybin, 1988) that in general case the transformation

$$\rho = \rho(\xi, t), \quad \mathbf{v} = \frac{\mathbf{r}}{\xi} V(\xi, t), \quad \nabla \varphi = 4\pi G \frac{\mathbf{r}}{\xi^3} \int_0^\xi \rho \xi'^2 d\xi'$$

brings the system (1) again to the form (2)–(4), where one should now replace

$$r \rightarrow \xi, \quad v \rightarrow V.$$

Thus, with this replacement, all our results hold for the ellipsoidal distributions as well.

Acknowledgement

This work was supported in part by INTAS through the grant 99-1068.

References

- Dwivedi, I. H. and Joshi, P. S. (1997). *Class. Quantum Grav.*, **14**, 1223.
 Gurevich, A. V. and Zybin, K. P. (1988). *Sov. Phys. JETP*, **67**, 1.
 Gurevich, A. V. and Zybin, K. P. (1995). *Uspekhi Fiz. Nauk*, **165**, 723.
 Gurevich, A. V., Zybin, K. P. and Sirota, V. A. (1997). *Uspekhi Fiz. Nauk*, **167**, 913.
 Hunter, C. (1962). *Astrophys. J.*, **136**, 594.
 Hunter, C. (1964). *Astrophys. J.*, **139**, 570.
 Lin, C. C., Mestel, L. and Shu, F. M. (1965). *Astrophys. J.*, **142**, 1431.
 Mestel, L. (1965). *QJRAS*, **6**, 161.
 Newman, R. P. A. C. (1986). *Class. Quantum Grav.*, **3**, 527.
 Papapetrou, A. and Hamoui, A. (1967). *Ann. Inst. Henri Poincare*, **6**, 343.
 Penston, M. V. (1969). *Mon. Not. R. Astron. Soc.*, **144**, 425.
 Pibbles, P. J. E. (1980). *The Large-Scale Structure of the Universe*. Princeton University, Princeton.
 Shandarin, S. F., Doroshkevich, A. G. and Zel'dovich, Ya. B. (1983). *Uspekhi Fiz. Nauk*, **139**, 83.
 Spitzer, L. Jr. (1978). *Physical Processes in the Interstellar Medium*. John Wiley and Sons, New York.
 Swatton, D. J. R. and Clarke, C. J. S. (1998). *Class. Quantum Grav.*, **15**, 2891.
 Zel'dovich, Ya. B. and Novikov, I. D. (1983). *The Structure and Evolution of the Universe*. University of Chicago, Chicago.

7 APPENDIX

Let us prove that the inequality (22) is the necessary and sufficient condition for arising the shell-crossing singularity.

The necessity follows obviously from the fact that when $0 < z \leq 1$ the function $P(z)$ in the Eq. (24) is less than unity.

To prove the sufficiency we first show that under the condition (22) the system (24). (26) has non-zero solutions. Geometrically, this means that the curves $z = z(m)$ and $z = \tilde{z}(m)$, determined by (24) and (26) correspondingly, cross each other on the plane (m, z) .

Consider the function $Y(m)$. From the definition (17) it follows that for non-singular initial distributions with a finite mass M the function $Y(m)$ is positive, differentiable in the region $0 < m < M$, and $Y(0) = 1, Y(m) \rightarrow +\infty (m \rightarrow M)$. Therefore, if the inequality (22) holds in some range of m , an interval $[m_1, m_2]$ will exist such that

$$Y(m) < 1 \quad (m_1 \leq m < m_2), \quad Y(m_2) = 1, \quad Y(m) > 1 \quad (m_2 < m < M),$$

$$Y'(m) > 0 \quad (m_1 < m < m_2), \quad Y'(m_1) = 0, \quad Y'(m_2) \geq 0$$

with $Y'(m_2) = 0$ when there is an inflection point at $m = m_2$. Hence

$$Y(m) \sim 1 + \alpha(m - m_2)^{2n+1} \quad (\alpha > 0, m \rightarrow m_2).$$

The function $P(z)$ in the right hand side of (24) is defined in the interval $0 \leq z \leq 1$ and decreases monotonically with $P(z) \sim 1 - (4/3\pi)z^3 (z \rightarrow 0), P(1) = 0, P'(1) = -6$ (see Fig. 2). Hence, in the interval $[m_1, m_2]$ the Eq. (24) determines uniquely a non-negative function $z = z(m)$. It is easy to see that

$$0 < z(m_1) < 1, \quad z'(m_1) = 0, \quad z'(m) < 0 \quad (m_1 < m < m_2), \quad z(m_2) = 0.$$

Consider now the Eq. (26). Its right hand side is defined in the interval $0 \leq z \leq 1$ and increases monotonically from zero at $z = 0$ to unity at $z = 1$ (Fig. 2). The left hand side of (26) is positive in $m_1 < m < m_2$ and becomes zero at $m = m_1$. Suppose, first, that it does not achieve unity anywhere in $[m_1, m_2]$. Then (26) determines a single-valued non-negative function $z = \tilde{z}(m)$ everywhere in $[m_1, m_2]$. Obviously, $\tilde{z}(m_1) = 0, 0 \leq \tilde{z}(m_2) < 1$ with $\tilde{z}(m_2) = 0$ if $Y'(m_2) = 0$. Taking into account the behaviour of $z(m)$ we hence conclude that if $0 < \tilde{z}(m_2) < 1$ then the curves $z = z(m)$ and $z = \tilde{z}(m)$ will necessarily cross each other on the plane (m, z) in the domain $m_1 < m < m_2, 0 < z < 1$. This statement holds with $\tilde{z}(m_2) = 0$ as well. Indeed, in this case from the behaviour of the functions $P(z)$ and $Y(m)$ as $z \rightarrow 0, m \rightarrow m_2$ it follows that

$$\frac{z(m)}{\tilde{z}(m)} \sim (m_2 - m)^{1/3} \rightarrow 0 \quad (m \rightarrow m_2),$$

and, hence, in the domain $m_1 < m < m_2, 0 < z < 1$ the intersection points exist again. Suppose now that in the interval $[m_1, m_2]$ the left hand side of (26) achieves unity for the first time at $m = m^* (m_1 < m^* < m_2)$. Then

$$0 < m (\ln Y(m))' < 1 \quad (m_1 < m < m^*),$$

so that the function $\tilde{z}(m)$ is uniquely defined in $[m_1, m^*]$ with $\tilde{z}(m^*) = 1$. It is clear that in this case the curves $z = z(m)$ and $z = \tilde{z}(m)$ have intersection points in the domain $m_1 < m < m^*, 0 < z < 1$.

Let us show that among the intersection points there are those which correspond to the minima of the function $\sigma(m, z)$ (12) on the curve $z = z(m)$. Consider the interval $[m_1, m_2]$.

As it follows from the above, it contains an odd number of values of m , abscissae of the intersection points, where the function $\sigma(m, z(m))$ has extrema. Let us calculate the derivatives of $\sigma(m, z(m))$ at the boundaries of the interval. With $z'(m_1) = 0$ and (16) we obtain

$$\left(\frac{d\sigma}{dm}\right)_{m_1} = \left(\frac{\partial\sigma}{\partial m}\right)_{m_1} = \frac{\sigma(m_1, z(m_1))}{2m_1}(Y(m_1) - 1) < 0.$$

Using (27), (28) and the asymptotic behaviour of $P(z)$ ($z \rightarrow 0$), $Y(m)$ ($m \rightarrow m_2$) we find

$$\left(\frac{d\sigma}{dm}\right)_{m \rightarrow m_2} \sim \frac{2}{\pi} t_f(m_2) Y'_{m \rightarrow m_2} \sim \alpha(m_2 - m)^{2n},$$

so that

$$\left(\frac{d\sigma}{dm}\right)_{m_2} > 0 \quad (n = 0), \quad \left(\frac{d\sigma}{dm}\right)_{m \rightarrow m_2} \rightarrow +0 \quad (n \geq 1).$$

It follows that $\sigma(z, z(m))$ has at least one minimum on $[m_1, m_2]$. This completes the proof.